Ultra-high magnetic field study of the Kondo-type zero-bias conductance peak in magnetically doped metal-insulator-metal tunnel junctions

Stuart Bermon
Department of Physics, City College of The City University of New York, New York, New York 10031

D. E. Paraskevopoulos and P. M. Tedrow
Francis Bitter National Magnet Laboratory, Massachusetts Institute of Technology, Cambridge, Massachusetts 02139
(Received 31 October 1977)

We have measured the zero-bias conductance peak in Al-*I*-Al tunnel junctions with Fe impurities incorporated into the insulator in magnetic fields up to 181 kG and at temperatures from 4.2 to 0.4 K. In zero field, the voltage and temperature dependence of the peak fits the Appelbaum theory quite well, providing a direct measure of the Kondo scattering amplitude in the perturbational limit. In high field, we have made a very careful comparison of the data to the Appelbaum theory modified to include the possibility of magnetic-field-induced lifetime broadening of the kind suggested by Wolf and Losee. We find that although it is possible at any given field to obtain a reasonable fit to the experimental line shapes, the fit at other fields becomes poor. The observed curves do exhibit an increased broadening with increasing magnetic field, but the deduced values of the broadening parameter Γ versus field do not agree with the predicted broadening based upon the measured g shift. The broadening can quantitatively account for the temperature dependence of the conductance in a given field, but fails to predict the observed dependence of the magnetoconductance at zero bias, in particular, the lack of saturation at very high magnetic field. No evidence is found for the existence of the type of triangular well observed in metal-semiconductor tunnel junctions at low temperatures.

I. INTRODUCTION

It is by now well established that the zero-bias peaks observed in the dynamic conductance of thin-film metal-insulator-metal tunnel junctions have their origin in the exchange scattering of the tunneling electrons from magnetic impurities in the insulating barrier region. These zero-bias conductance peaks, first observed in *M-I-M* junctions by Wyatt[1] (Ta-*I*-Al), are typically on the order of several millivolts wide and characterized by a logarithmic dependence on voltage (for $eV \gg kT$), and at zero bias by a logarithmic dependence on temperature. In addition to junctions made with transition-metal electrodes (Ta and Nb),[1-3] the effect has also been studied in tunnel junctions like[4-8] Al-*I*-Al and[9,10] Al-*I*-Ag in which the insulator has been intentionally doped with controlled amounts of magnetic impurities such as Cr,[5] Fe,[7] and Ti,[8,11] thus allowing a study of the dependence of the peak behavior on the impurity concentration. A third type of system in which such conductance peaks are observed consists of metal-semiconductor tunnel junctions[12-14] in which the localized magnetic states are thought to be lightly screened neutral donors at the inner edge of the depletion region.

The exchange scattering which gives rise to the conductance peak is of the same kind that is responsible for the anomalous log$T$ dependence of the resistivity in dilute magnetic alloys commonly referred to as the Kondo effect.[15] Using this idea as a basis, Appelbaum[16] considered the effect of adding to the usual tunneling Hamiltonian an extra phenomenological term

$$H_{T_J} = T_J \sum_{l,r,\sigma,\sigma'} \vec{S}\cdot\vec{\tau}_{\sigma\sigma'}(a^\dagger_{l\sigma}b_{r\sigma'} + b^\dagger_{r\sigma'}a_{l\sigma}), \tag{1}$$

which transfers electrons across the barrier with spin flip. Here $a_{l\sigma}$ ($a_{r\sigma}$) refer to the destruction operator for an electron with momentum l (r), and spin state σ on the left- (right-) hand side of the barrier. $\vec{\tau}_{\sigma\sigma'}$ is the Pauli spin operator, $\vec{S}$ the spin of the localized magnetic state, and T_J an undetermined matrix element assumed to be constant. This term is in addition to the usual exchange term

$$H_J = -J \sum_{l,l',\sigma,\sigma'} \vec{S}\cdot\vec{\tau}_{\sigma\sigma'}a^\dagger_{l\sigma}a_{l'\sigma'}, \tag{2}$$

which scatters an electron from the impurity back into the electrode. In zero magnetic field, to second order in perturbation theory, a voltage and temperature-independent extra conductance was found (hereafter referred to as $G^{(2)}$), but in third order, Appelbaum calculated an extra conductance term of the form

$$G^{(3)} = -A\int_{-\infty}^{\infty} F(\epsilon)\frac{\partial f(\epsilon - eV)}{\partial \epsilon}\, d\epsilon, \tag{3}$$

with

$$F(\epsilon) = \int_{-E_0}^{E_0} \frac{1-2f(\epsilon')}{\epsilon'-\epsilon}\, d\epsilon' = \int_{-E_0}^{E_0} \frac{\tanh(\epsilon'/2kT)}{\epsilon'-\epsilon}\, d\epsilon', \quad (4)$$

where A is a constant, f is the Fermi function, and E_0 is a cutoff parameter. Now $F(\epsilon)$ in Eq. (4) is precisely Kondo's[15] result for the energy dependence of the scattering amplitude in third-order perturbation theory. $\partial f/\partial\epsilon$ in Eq. (3) is just a bell-shaped curve of width $\sim 3.5kT$ centered around $\epsilon = eV$ which, for sufficiently low temperature, acts as a fine probe of $F(\epsilon)$. Thus aside from the thermal smearing described by Eq. (3), $G^{(3)}(V)$ should directly measure the energy dependence of the Kondo scattering amplitude, at least in the perturbational limit.

Detailed comparisons of the observed voltage and temperature dependences of the conductance peaks in M-I-M junctions with a numerical evaluation of $G^{(3)}(V,T)$ by Appelbaum and Shen,[3] and by Wyatt and Wallis,[10] show good agreement with the zero-field theory. Wolf and Losee[12] fitted their results for Schottky-barrier tunnel junctions with an approximate interpolation function for $G^{(3)}$ of the form

$$G_I^{(3)} = -A \ln\{[(eV)^2 + (nkT)^2]/E_0^2\}^{1/2}, \quad (5)$$

where n and E_0 were taken as adjustable parameters for each temperature, but an average value of $n = 2.12$ was obtained. On the other hand, Nielsen[5] was not able to fit his data on a variety of doped M-I-M junctions unless an additional parameter γ^2 was added to the terms in the square brackets in Eq. (5).

A significant advance over Appelbaum's first calculation[16] was made by Appelbaum and Brinkman[17] using their previously obtained[18] Green's function formalism derived several years earlier by Zawadowski[19] by a different method. In this formulation the problem is divided into separate left- and right-hand Green's functions, and the tunneling current expressed in terms of these Green's functions and their spatial derivatives. The advantage of the method is that it contains no unknown phenomenological parameters such as T_J, and explicitly allows the dependence of the $G^{(2)}$ and $G^{(3)}$ terms on the position of the impurity in the barrier and/or electrode to be calculated. To third order, they found a similar voltage dependence to that predicted by Eqs. (3) and (4) with the sign of the $G^{(3)}$ term for $J<0$ predominantly positive (i.e., a conductance peak) for the impurity in the barrier but an oscillating function of position for the impurity in the metal electrode. In a similar calculation, Mezei and Zawadowski[20] investigated the effect of placing the impurity in the electrode but explicitly taking into account the momentum dependence of the exchange coupling integral $J_{\vec{k}\vec{k}'}$, in the s-d Hamiltonian. In addition to the oscillating term, they found a nonoscillating term whose effect is to depress the local density of states at the interface and to give a *resistance* peak about zero bias. The effect of placing impurities into the electrode has been recently investigated in films condensed onto liquid-helium-cooled substrates by Bermon and So.[21] In an earlier calculation, Solyom and Zawadowski[22] obtained a resistance peak (for $J<0$) for the impurity in the barrier because they had neglected the real part of the unperturbed Green's function. The situation has been recently clarified by Ivezic,[23] who, using the hopping model of tunneling proposed by Caroli *et al.*,[24] showed that the theories of Appelbaum and of Zawadowski are limiting cases of this model, valid when the impurity is close to the barrier-electrode interface, but not when the impurity is located sufficiently close to the center of the barrier *to sample the self-energies of both electrodes simultaneously* — a situation which, because of the different Fermi levels on each side of the barrier, constitutes a true nonequilibrium problem.

An important test of the theory is whether it can predict the magnetic field dependence of the conductance peak. The effect of a field is to split the spins into their Zeeman levels, so that now an electron undergoing spin-flip scattering must exchange the energy $\Delta = g\mu_B H$ necessary to place the impurity in an excited state. As a result, some of the processes that give an increased conductance in zero field are quenched out for $|eV| < g\mu_B H$. Appelbaum[16] calculated that the second-order $G^{(2)}$ term, which is voltage and temperature independent in zero field, develops a conductance well centered about zero bias of width $2g\mu_B H$ whose sides are smeared by finite temperature by an amount $\sim 3kT$. The limiting depth of the well at high field is $1/(S+1)$ of the zero-field value of $G^{(2)}$, where S is the spin of the impurity. In third order, the Kondo peak splits into three peaks, one remaining centered at zero, one shifted toward positive voltage by $eV = g\mu_B H$, and one shifted toward negative voltage by a similar amount. The center peak is multiplied by a smeared square well similar to that for $G^{(2)}$ (but whose limiting high-field value is zero) and is not seen. The right- and left-hand peaks are multiplied by right- and left-hand step functions (smeared by $\sim 3kT$) centered at $eV = g\mu_B H$ and $-g\mu_B H$, respectively. The result is to produce a conductance well straddled by a double-peaked structure that causes the conductance in high field to exceed the zero-field conductance for $eV > g\mu_B H$. The existence of this "overshoot" is an important verification of the predicted[16]

magnetic-field-induced splitting of the $G^{(3)}$ term.

Shen and Rowell[2] studied Ta-I-Al and Sn-I-Sn junctions in fields up to 40 kG and at 1.5 K. They observed a conductance well but no indication of any overshoot behavior and analyzed their data purely in terms of the depression in the conductance of the $G^{(2)}$ term alone. Lythall and Wyatt[9] applied 42 kG at 1.3 K to a Cr-doped Al-I-Ag junction. Nielsen[25] reported measurements of a Ti-doped Al-I-Al junction at 1.3 K and 150 kG. Bermon and Ware[7] measured the field-induced conductance well in Fe-doped Al-I-Al junctions as a function of Fe concentration in fields up to 80 kG at 1.12 K. Appelbaum and Shen[3] made a quantitative comparison to the theory of their results for Ta-I-Al junctions at 0.3 K and 90 kG, and more recently Wallis and Wyatt[26] presented an analysis of data they obtained for Ti-doped Al-I-Ag junctions measured at 4.2 and 1.4 K, in fields up to 70 kG. In the case of metal-semiconductor tunnel junctions extensive magnetic field measurements were made by Wolf and Losee[12] (WL) up to 150 kG at temperatures down to 1.25 K.

In all the above cases, the observed shape of the conductance well was never that of a slightly smeared ($\sim 3kT$) rectangular well, but that of a much more broadened well, resembling a U or rounded-V shape. Furthermore, the aforementioned overshoot behavior caused by the splitting of the Kondo peak in third order was only observed in two instances: in Fe-doped Al-I-Al (Ref. 7) and in Ta-I-Al (Ref. 3) junctions, and to an extent was considerably smaller than predicted by Appelbaum's theory.

Wolf and Losee[12] attempted to explain the large smearing and lack of overshoot in their curves by introducing a magnetic-field-induced lifetime broadening of the Zeeman transition of the local moment occurring via the exchange interaction. This inherent lifetime broadening of the Zeeman levels is given by the expression[27,28]

$$\Gamma = \pi(J\rho)^2\Delta , \tag{6}$$

where $\Delta = g\mu_B H \gg kT$, ρ is the density of states of one-spin index at the Fermi surface, and J is the exchange coupling constant. This broadening must also, according to WL, be taken into account in the third-order scattering calculation as it broadens the intermediate spin-flipped states, and for $\Gamma \gg kT$ reduces the Kondo scattering peak from $-\log T$ to $-\log\Gamma/k$. They further pointed out that there should be a g shift (analogous to the Knight shift in NMR), due to the fact that the conduction-electron spins polarize in an applied field H, which is given by

$$g = g_0 + 2J\rho , \tag{7}$$

where g_0 is the g value for the local moment in the absence of exchange coupling. Thus, in principle, by measuring the width of the well to obtain Δ and determining $g - g_0$ (they assumed $g_0 = 2$), one could determine the exchange coupling parameter $J\rho$ from Eq. (7), and in turn, from Eq. (6), the lifetime broadening Γ which value could be compared with the actually observed smearing of the well. From the standpoint of consistency with the perturbation theory, WL's $J\rho$ values determined in this way were extraordinarily high (~ -0.5), but they claimed good agreement between their measured Γ's and the values calculated from their measured g shifts using Eqs. (6) and (7).

Rowell and Tsui[13] and Bermon *et al.*,[14] however, found that when the measurements on this type of junction were extended to lower temperature, the well took a V shape rather than that of a smeared rectangular well. In particular, Bermon's[14] measurement at 0.03 K and 80 kG showed the well to be accurately triangular with a definite cusp at zero voltage. Now a calculated broadening parameter based on an ideal well that is rectangular would be very different from one deduced assuming the idealized well was triangular in shape. Furthermore the presence of the cusp at zero calls into question the whole idea of the existence of any significant broadening mechanism in high field.

In the fields and temperatures measured so far, M-I-M junctions do not appear to exhibit the above described triangular-well behavior characteristic of the metal-semiconductor junctions. It is the purpose of this work to extend the tunneling measurements in intentionally doped M-I-M junctions to combinations of field and temperatures previously not available, and to make a more careful and detailed comparison with the WL-modified Appelbaum theory than has heretofore been attempted.

II. EXPERIMENTAL PROCEDURE

Junctions were prepared in a Varian-NRC 6-in. oil-diffusion–pumped-vacuum system at base pressures of 0.5 to 1.0×10^{-6} Torr. The substrates, which were of Corning 7059 glass selected for its extremely smooth surface, were first cleaned with a hot detergent solution, rinsed with distilled water, and vapor degreased in acetone or isopropyl alcohol. Gold-film electrodes backed by Al were evaporated for electrical contact. The bottom strip of Al, approximately 1200 Å thick and $\frac{1}{8}$ in. wide, was evaporated either from a boron nitride crucible or by electron beam, and then a 1000-Å film of SiO was deposited to cover the edges and

reduce the exposed portion of the Al to a strip 0.8 mm wide. The Al was then exposed to room air for approximately 10–16 h, while being heated to about 100 °C to promote oxidation. After the system had been reevacuated, the Al was heated an additional 30 min at 10^{-6} Torr to expel any absorbed water vapor which might enhance the oxidization of the deposited iron. The iron itself, which was in the form of 0.030-in.-diam wire was etched in HNO_3, rinsed with acetone and immediately inserted in the vacuum chamber. Evaporation was from tungsten boats at about 0.3 Å/sec through a motor-controlled rotating sectored-shutter mask, similar to that used previously by Bermon and Ware,[7] that allowed different amounts of Fe to be evaporated onto the insulating layers of the seven junctions on each side of the substrate. Film thicknesses and evaporation rates were measured with a calibrated quartz-crystal thickness monitor. The junctions were completed by evaporating Al cross strips, 1 mm wide and 1200 Å thick. The length of time that the Fe was exposed to the vacuum system before the deposition of the top Al layer varied between 20 sec and 3 min. No consistent dependence of the conductance-peak height on this time interval was observed.

The low-temperature measurements were made in the range from 4.2 to 0.40 K using a ^{3}He refrigerator with the sample immersed directly in the ^{3}He liquid below 2.5 K and in the vapor above that temperature. Temperatures were determined from a carbon resistor calibrated against the vapor pressures of ^{3}He and ^{4}He, and controlled by a heater and an electronic feedback circuit capable of a temperature stability of $\lesssim$0.001 K. The magnetic field measurements were made in the axial fields of two separate Bitter electromagnets, one capable of fields up to 150 kG and the other to 181 kG. The field was set parallel to the plane of the junction, although results are independent of field orientation.

Derivative measurements were made in the usual manner by applying a small ($\lesssim$100 μV) constant-current ac signal to the junction, and measuring the resultant ac output voltage as a function of the applied dc bias voltage. The zero offset capability of the lock-in amplifier was used to expand the curves to full scale, with a stability and resolution of better than 0.01%. dV/dI values taken directly from the plotted curves were converted to $G = dI/dV$ and $G_{\text{even}} = \frac{1}{2}[G(V) + G(-V)]$ by computer.

Below the superconducting transition temperature of Al the junctions always exhibited the expected superconducting gap behavior, and for the "zero-field" measurements below 1.25 K, a small magnetic field of from 1.5 to 2.5 kG was applied to keep the Al in its normal state.

III. RESULTS AND DISCUSSION

The measurements reported here were all performed on one junction of Fe-doped Al-Al_2O-Al with the mass equivalent of 1.5 Å of Fe evaporated onto the insulator, which is equivalent to about 0.4 of a statistical monolayer of Fe. At this concentration, the amplitude of the conductance peak and the depth of the field-induced well are approximately at a maximum, but the voltage and temperature dependence of the zero-field conductance still follow closely the predictions of the perturbational calculation [Eqs. (3) and (4)]. Significantly higher concentrations were avoided due to clearly observed deviations from the zero-field Kondo result. Comparison of the present curves for $H \leq 80$ kG and $T \geq 1.12$ K show good agreement with data collected in that range on previously fabricated Fe-doped junctions by Bermon and Paraskevopoulos,[29] and Bermon and Ware,[7] the difference being in the height of zero-bias conductance peak above the background conductance. In the present samples it is approximately 5%–10% higher at a given concentration.

A. Zero-field results

Figure 1 shows a plot of the dynamic resistance dV/dI versus voltage bias V for $T = 4.2$ K in the range $|V| \lesssim \pm 25$ mV. This extended range is displayed to indicate the behavior of the background resistance shown by the dashed line in the figure. This background resistance is obtained by computer fitting the best offset parabola

$$R_B(V) = R_M - b(V - V_M)^2$$

(where R_M, V_m, and b are coefficients to be determined) to the resistance curve in the voltage range beyond the conductance peak. This procedure de-

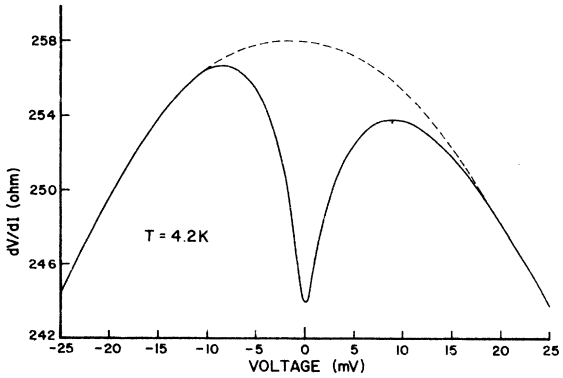

FIG. 1. Dynamic resistance vs bias voltage for an Fe-doped Al-I-Al tunnel junction showing extrapolated parabolic background resistance (dashed curve). Voltage is measured with respect to the bottom Al film.

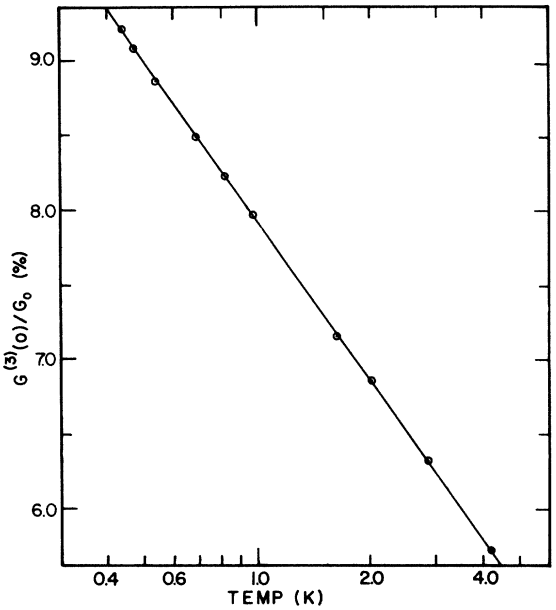

FIG. 2. Conductance at zero bias plotted as a function of temperature for an Fe-doped Al-I-Al tunnel junction. The background conductance $G_0 \equiv G_B(V=0)$ has been subtracted out and the difference normalized to G_0 as explained in the text.

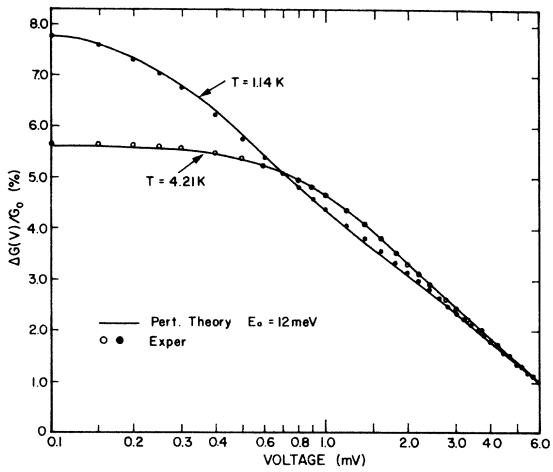

FIG. 3. Semilog plot of the zero-field voltage dependence of the even part of the dynamic conductance of an Fe-doped Al-I-Al tunnel junction compared with the computed conductance (solid lines) using Kondo's perturbational result, Eqs. (3) and (4). The background conductance has been subtracted and the difference normalized to $G_0 \equiv G_B(0)$.

termines the height of the conductance peak, and thus the size of the $G^{(3)}$ term, and to some extent influences the functional dependence of the peak, although the effect of the variation in the background over the range of measurement for the magnetic field curves (±3.5 mV) is small (less than ±0.1% compared to a peak height of 9% for $T = 0.4$ K). Below 4.2 K there is no temperature variation of the background, and so the functional behavior of the temperature dependence of the peak at zero bias becomes independent of assumptions about that background.

Figure 2 shows the temperature variation of the difference between the zero-bias conductance and the background conductance, normalized to the background conductance $G^{(3)}(0) = [G(0) - G_0]/G_0$, in the temperature range from 4.2 to 0.40 K. The dependence, which is seen to be logarithmic, in accordance with the Appelbaum-Kondo prediction [Eqs. (3) and (4)], indicates that we are still in the perturbational regime at the lowest temperature of measurement, and the particular assumptions of the perturbation theory in treating the magnetic field case should still be valid. It should be pointed out, however, that the small magnetic field (of up to 2.5 kG) applied to the junction to keep the Al in the normal state should produce a slight reduction in the conductance, increasing as the temperature is lowered, which, according to our study of the zero-bias magnetoconductance curves extrapolated to zero field, could amount to as much as 0.1%–0.2% at 0.4 K. Thus the slope of the line in Fig. 2 in true zero field would be somewhat steeper than that shown. In any case the dependence is not less than $-\log T$.

Figure 3 shows the *voltage* dependence on a semilog plot of the even part of the difference between the conductance and the background conductance $G_{\text{even}}(V) = [\Delta G(+V) + \Delta G(-V)]$ normalized to G_0 (the background conductance at zero bias) for $T = 4.21$ and 1.14 K. [Note that in this and in all later figures the subscript "even" on $G_{\text{even}}(V)$ has been suppressed; $G(V)$ always means the even conductance.] The points are the experimental values and the solid lines are the result of an exact numerical evaluation of $G^{(3)}(V)$ from Eqs. (3) and (4), with a fitted value of E_0 of 12 meV. The fit is quite good. Similar curves obtained at four intermediate temperatures (not shown) show at least as good a fit as those in Fig. 3. Additional low-field plots (on a linear scale) at 0.4 and 1.25 K are shown in Figs. 7–9 and 13 in connection with the discussion of the magnetic field behavior.

The values of the coefficient A in Eq. (3) and E_0 in Eq. (4) were obtained by fitting the experimental curve at one temperature in the region from approximately 1 to 3 mV, where both the theoretical and experimental dependences are closely logarithmic. Neither parameter was allowed to vary for different temperatures, as has been the case in some previous work. A word is in order about the fitted value of E_0. E_0 is a cutoff parameter introduced to prevent the integral in Eq. (4) (the de-

rivation of which assumes that the exchange coupling integral $J_{\vec{k}\vec{k}'}$ is a constant equal to J) from becoming divergent, and does not represent an actual physical cutoff such as might arise from the energy dependence of $J_{\vec{k}\vec{k}'}$ or of the density of states $\rho(\epsilon)$. As Appelbaum and Shen[3] have pointed out, for $\epsilon \ll E_0$, the only effect of varying E_0 is to introduce a constant term into the $G^{(3)}$ conductance varying as $\ln E_0$, a term which could be absorbed into the background conductance. They arbitrarily chose E_0 as 10 meV, and by fitting the zero-field curve in the range from 0.5 to 1.5 mV arrived at a value of A, thereby essentially fixing the magnitude of the $G^{(3)}$ term. In zero field, whether the constant conductance is included in $G^{(3)}$ or in the background is of no importance in analyzing the voltage behavior, but in high field the relative size of the $G^{(2)}$ term and $G^{(3)}$ term is quite important in determining the shape and depth of the field-induced well. This point has been discussed by Wallis and Wyatt.[26] In our procedure, the size of $G^{(3)}$ is determined by comparison of the measured conductance to the extrapolated parabolic background indicated in Fig. 1, which results, in effect, in making $G^{(3)}$ and hence its contribution to the field dependence as small as possible (i.e., any added constant conductance in $G^{(3)}$ is assumed to be zero). This fixing of the amplitude of $G^{(3)}$ then in turn determines E_0. We caution the reader that the value of E_0 determined in this way is only a convenient fitting parameter, and cannot necessarily be taken as a measure of some true physical cutoff, as for instance in the familiar formula

$$kT_K \simeq E_0 e^{-1/J\rho}$$

for the Kondo temperature T_K, as has been done by some authors.[12,26] Our numerical studies of the voltage dependence of $G^{(3)}$ from Eqs. (3) and (4) indicate that it does not begin to show the downward deviation from logarithmic behavior indicative of the negative singularity at $eV = E_0$ until $eV > \frac{1}{2}E_0$. Thus the comparison to the theory is not taken beyond 6 mV despite the fact that the experimental voltage dependence is still logarithmic for several millivolts past this value.

We have not compared our results with the interpolation function of Eq. (5) as we have found that the experimental curves actually constitute a considerably better fit to the exact calculation of $G^{(3)}$ from Eqs. (3) and (4) than does the interpolation function (for fixed n and E_0) itself. In particular, as Wyatt and Wallis have pointed out,[10] the crossover behavior that occurs in the curves in Fig. 3 as the temperature is raised cannot be reproduced by the interpolation function. With an essentially exact expression for $F(\epsilon)$ in Eq. (4) available in terms of the digamma function from the paper by Bloomfield and Hamann,[30] there is really no good reason to continue to use an interpolation function that is a poorer approximation to the theory than are the observed experimental curves themselves.

B. High magnetic field results

Our results in high field are compared with the perturbation theory of Appelbaum[16] modified to include the possibility of magnetic-field-induced lifetime broadening as suggested by WL.[12] Appelbaum's results may be written in the following form[3]

$$G = G^{(1)}(V) + G^{(2)}(V) + G^{(3)}(V), \tag{8}$$

where

$$G^{(n)}(V) = -\int_{-\infty}^{\infty} g_n(\epsilon) \frac{\partial f(\epsilon - eV)}{\partial \epsilon}\, d\epsilon . \tag{9}$$

$g_1(\epsilon)$, $g_2(\epsilon)$, and $g_3(\epsilon)$ are the first-, second-, and third-order terms, respectively, before smearing by the derivative of the Fermi function in Eq. (9), and are given by

$$g_1(\epsilon) = A_1 , \tag{10}$$

$$g_2(\epsilon) = A_2\left[1 + \frac{\langle M\rangle}{2S(S+1)}\left(\tanh\frac{\Delta+\epsilon}{2kT} + \tanh\frac{\Delta-\epsilon}{2kT}\right)\right], \tag{11}$$

$$g_3(\epsilon) = A_3[g_{31}(\epsilon) + g_{32}(\epsilon) + g_{33}(\epsilon)], \tag{12}$$

$$g_{31}(\epsilon) = \frac{1}{2}\left[1 - \frac{\langle M^2\rangle}{S(S+1)} + \frac{\langle M\rangle}{2S(S+1)} \times \left(\tanh\frac{\Delta+\epsilon}{2kT} + \tanh\frac{\Delta-\epsilon}{2kT}\right)\right] F(\epsilon), \tag{13}$$

$$g_{32}(\epsilon) = \frac{1}{4}\left(1 + \frac{\langle M^2\rangle}{S(S+1)} + \frac{\langle M\rangle}{S(S+1)} \tanh\frac{\Delta+\epsilon}{2kT}\right) F(\epsilon + \Delta), \tag{14}$$

$$g_{33}(\epsilon) = \frac{1}{4}\left(1 + \frac{\langle M^2\rangle}{S(S+1)} + \frac{\langle M\rangle}{S(S+1)} \tanh\frac{\Delta-\epsilon}{2kT}\right) F(\epsilon - \Delta). \tag{15}$$

$F(\epsilon)$ is the Kondo integral given by Eq. (4), $\Delta = g\mu_B H$ is the Zeeman energy, $\langle M\rangle$ is the average spin polarization of the impurity in a field H defined so that it approaches $-S$ for high field, and $\langle M^2\rangle$ is the average of the square of the spin polarization,

$$\langle M\rangle = \tfrac{1}{2}\coth(\Delta/2kT) - (S+\tfrac{1}{2})\coth(S+\tfrac{1}{2})(\Delta/kT), \tag{16}$$

$$\langle M^2\rangle = \langle M\rangle^2 - (S+\tfrac{1}{2})\operatorname{csch}^2(S+\tfrac{1}{2})\frac{\Delta}{kT} + \tfrac{1}{4}\operatorname{csch}^2\frac{\Delta}{2kT} . \tag{17}$$

The adjustable parameters A_n are defined differently from those of Appelbaum and Shen,[3] in that

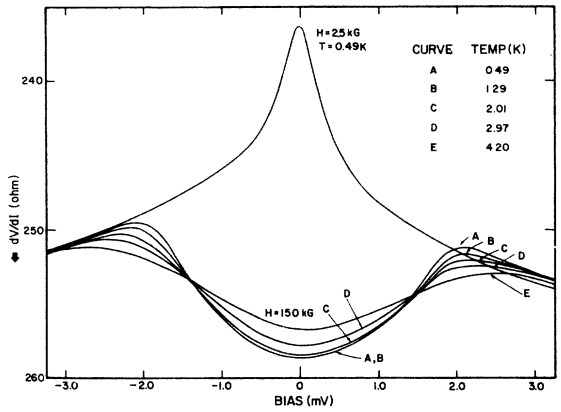

FIG. 4. Dynamic resistance of an Fe-doped Al-*I*-Al tunnel junction (shown plotted downward to resemble the conductance) as a function of bias voltage for fixed magnetic field (150 kG) and variable temperature. Also shown is the "zero field" (actually 2.5 kG) curve at the lowest temperature for comparison.

in zero field $g_2(\epsilon)=A_2$ and $g_3=A_3F(\epsilon)$, where A_3 is the same as the coefficient A in Eq. (3).

The tanh functions in the above expressions, which have slope $1/2kT$ at $\epsilon=\pm\Delta$, in combination with the kT smearing of Eq. (9) are what principally determine the smearing of the sides of the well. Even a cursory inspection of the experimental curves presented in Figs. 4 and 6, reveals that the observed well smearing greatly exceeds that predicted by the theory ($3kT$ at 0.4 K is only about 0.1 meV). As already explained, in order to account for an apparently similar broadening in their semiconductor junctions, WL[12] introduced the lifetime broadening parameter Γ [Eq. (6)]. One of the effects of this broadening would presumably be to introduce an energy uncertainty into the spin-flipped intermediate states in the Kondo third-order perturbational calculation. Suhl[31] had previously suggested (in discussing the effect of interactions on the Kondo effect) that for a distribution $R(\epsilon)$ of intermediate-state energies the function $\tanh(\epsilon/2kT)$ in the Kondo integral [Eq. (4)] should be replaced by the convolution

$$S(\epsilon)=\int_{-\infty}^{\infty} R(\epsilon')\tanh\frac{\epsilon-\epsilon'}{2kT}\,d\epsilon'. \tag{18}$$

WL took for $R(\epsilon)$ a Lorentzian function

$$R(\epsilon)=(\Gamma/\pi)/(\Gamma^2+\epsilon^2), \tag{19}$$

which, when substituted into Eq. (18), leads in the limit $\Gamma\gg kT$ to a broadening of the steplike tanh function at $\epsilon=0$ (step width $\sim kT$) to a steplike $\tan^{-1}$ step function of width $\sim\Gamma$, thus reducing the Kondo peak from a $-\log kT$ to a $-\log\Gamma$ dependence. In addition, the effect of the broadening on the threshold for Zeeman excitation is included by similarly convoluting the tanh functions everywhere they appear in g_2 and g_3.

In this paper, we follow a simpler procedure suggested by Appelbaum and Shen,[3] who introduced an effective temperature T^* to simulate the smearing of the $\tanh\epsilon/2kT$ functions in g_n, $F(\epsilon)$, and the coth functions in $\langle M\rangle$ by replacing T in these expressions with T^*, where, for $\Gamma\gg kT$, $T^*\simeq\Gamma/k$. The T in the Fermi function of Eq. (9), which represents the electron distribution in the metals, remains unchanged, however. The principal advantage of this procedure is that by substituting the numerical evaluation of a single integral for that of a triple integral in WL's method, it reduces the required computation time by almost three orders of magnitude (according to our studies) and makes feasible the idea of determining the values of the desired parameters such as the g factor, Γ, etc. by a process of curve fitting rather than by simply identifying various critical points of the curves, which, as will be seen, can lead to substantial error. Appelbaum and Shen[3] considered only the case where the external broadening was much greater than the thermal broadening, $\Gamma\gg kT$, so that $kT^*\simeq\Gamma$. Where the temperature is sufficiently high or Γ sufficiently small that the extra broadening is comparable to the thermal smearing already present, the appropriate expression that relates T^* to Γ is[31]

$$kT^*=[(kT)^2+\Gamma^2]^{1/2}. \tag{20}$$

For convenience, we shall adopt the convention of expressing Γ not in meV, but in temperature units, to make comparison with the actual temperature and T^* easier.

Figure 4 shows the measured derivative curves at the fixed field of 150 kG for temperatures ranging from 0.49 to 4.20 K. Also plotted is the "zero-field" (actually 2.5-kG) curve for the lowest temperature. Following Rowell, we plot dV/dI upside-down to make comparison with theoretically calculated conductances easier. Noting that at 0.49 K, $3kT\simeq0.13$ mV, we observe immediately that the low-temperature curves are severely broadened, and despite the fact that the ratio of the highest and lowest temperatures is about 9, the ratio of the slopes of wells of the corresponding curves is only about 3. In Fig. 5(a) are shown the conductance curves calculated from the unsmeared Appelbaum theory for the same field and temperatures of Fig. 4. The Zeeman energy $\Delta=1.72$ meV corresponds to a g value of 1.98. The theoretical line shapes bear little resemblance to the experimental. The theory can be much more closely brought into agreement with experiment by including the broadening parameter $\Gamma=3.44$ K (obtained by fitting the lowest-temperature curve) as indicated in Fig. 5(b). The sharpness of the well

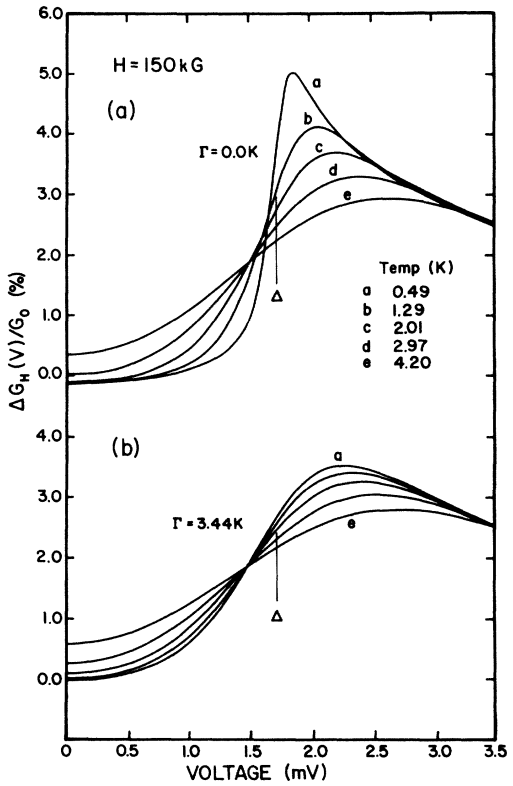

FIG. 5. Theoretical dynamic conductance from the Appelbaum theory for fixed field and the same temperatures as in Fig. 4 calculated for (a) no extra broadening ($\Gamma = 0.0$ K), and (b) with a broadening parameter of the kind suggested by Wolf and Losee, $\Gamma = 3.44$ K, selected to match the experimental behavior. The value of the Zeeman energy ($\Delta = g\mu_B H = 1.72$ meV) is also indicated and is seen to lie significantly above the voltages at which the slopes of the theoretical curves are a maximum, and above the pivot point of the curves.

at the lower temperatures is of course considerably reduced, as is the overshoot for $eV \gtrsim \Delta$. The change in the slope of the well with temperature now reasonably reproduces the experimental behavior. At this point, Figs. 4 and 5 are presented to provide a qualitative comparison only. A quantitative comparison of the temperature dependence of exact experimental even conductances with the theory will be made further on.

Figure 5 does serve, however, to illustrate an important point that has generally been ignored in previous work, namely, that in the theory, at least for the $G^{(3)}$ terms comparable in size to the $G^{(2)}$, the value of the Zeeman energy $\Delta = g\mu_B H$ is *not* obtained by determining the voltage at which the slope of the conductance well is a maximum. Only in the presence of $G^{(2)}$ alone would this be true. $G^{(3)}$ involves the multiplication of the steplike $\tanh[(\epsilon \pm \Delta)/2kT]$ function which has maximum slope at $\epsilon = \pm\Delta$, with the shifted Kondo peak which has slope zero at $\epsilon = \pm\Delta$. The combination of the two produces a maximum in the derivative of $G^{(3)}$ occurring at some 15%–25% below the voltage corresponding to Δ over the range of temperatures and fields measured here. With the inclusion of $G^{(2)}$ the shift is reduced, but can still easily be 10%–15%. Considering that even an error of 10% would lower an actual g value of say 1.95 to an estimated value of 1.75, and by Eq. (7) change the computed value of $J\rho$ by a factor of 5 (assuming $g_0 = 2$), this discrepancy in the determination of Δ cannot be ignored. Likewise, the determination of Γ by taking the voltage interval in which dG/dV decreases from its peak value to half that value[12] is only reasonably accurate in the presence of $G^{(2)}$ alone, but not with a significant amount of $G^{(3)}$ mixed in.

We have adopted the procedure of using the theory to try to obtain the best possible fit to the experimental data and deducing the values of the various parameters such as g and Γ from that fit. The principal set of experimental curves used as the basis for analysis is shown in Fig. 6, which exhibits the derivative curves for the lowest temperature measured ($T = 0.4$ K) in fields of 2.5, 40, 80, 110, 149, and 181 kG, respectively. For each field, the dV/dI curve was digitized, converted to conductance $G(V)$, the background conductance subtracted to give $\Delta G(V)$, and the even conductance $\Delta G_H(V) = \frac{1}{2}[\Delta G(+V) + \Delta G(-V)]$ extracted. The curve was then divided by the background conductance at zero bias $[G_0 \equiv G_B(V=0)]$ and expressed as a percentage. Thus 0.0% on the vertical axis represents the background level, which by the above procedure is automatically normalized to the value 100 for all plots.

The parameter A_3 of Eq. (12) was determined, as already outlined in Sec. III A, by fitting the low-

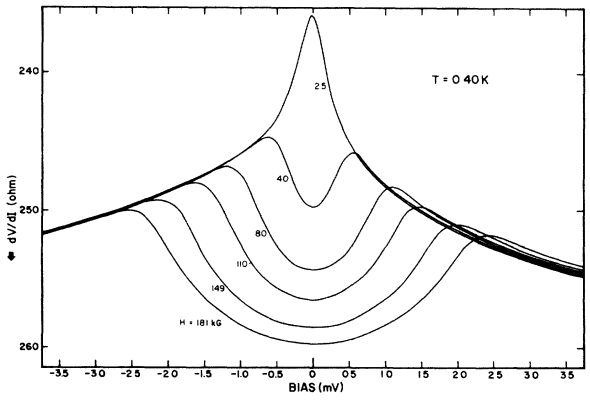

FIG. 6. Dynamic resistance of an Fe-doped Al-*I*-Al tunnel junction (shown plotted downward to resemble the conductance) as a function of bias voltage for the lowest measured temperature in fields up to 181 kG.

field curve at $V = 1.4$ mV and adjusting E_0 to give the best fit in the logarithmic range from 1 to 3 mV, avoiding the field- and temperature-sensitive region about zero bias. A_2, which determines the ratio of the $G^{(2)}$ to the $G^{(3)}$ term, was fixed principally by the depth of the well, by matching the conductance curve in the vicinity of $eV \simeq \frac{1}{3}\Delta$. Since the "background" conductance in zero field is the sum of $G^{(1)}$ and $G^{(2)}$ (here made to be 100), A_1 is just $100 - A_2$. The g factor was then determined by fitting the width of the well for the given field, and the broadening parameter Γ by best matching the slope of the well in the vicinity of Δ. The shape of the well is relatively insensitive to the precise value of the spin S, although different choices of S will change the value of A_2. For lack of better information, we have chosen $S = 2$, which corresponds to the spin of the free Fe atom.

The results of such a procedure are shown for the single intermediate field $H = 110$ kG in Fig. 7 along with the low-field ($H = 2.5$ kG) curve. The solid lines are the experimental curves, and the dashed theoretical, with the curve labeled $\Gamma = 0$ the Appelbaum result with no additional broadening. To match the slope of the well, the value of $\Gamma = 2.75$ K (0.237 meV) is required. The fitted value of g is 1.98 ($\Delta = 1.26$ meV), while $A_3 = 1.80$ and $A_2 = 6.45$. Over most of the well the fit is quite good, although it starts to deteriorate beyond $V = 1.3$, with the experimental curve failing to reproduce the predicted overshoot behavior for $eV > \Delta$ of even the broadened theoretical curve by a significant margin. Although the quality of the fit over the majority of the well region is encouraging, the danger of making a comparison of the complete voltage curve to the theory at only one magnetic field[3] is illustrated by the graphs in Fig. 8. Here are shown the experimental curves (solid lines) for the five indicated fields in comparison with the theoretical curves (dashed) calculated using the values of A_2, A_3, and g derived from the fit to the 110-kG curve of Fig. 7, but with the value of Γ having been adjusted for each field to match

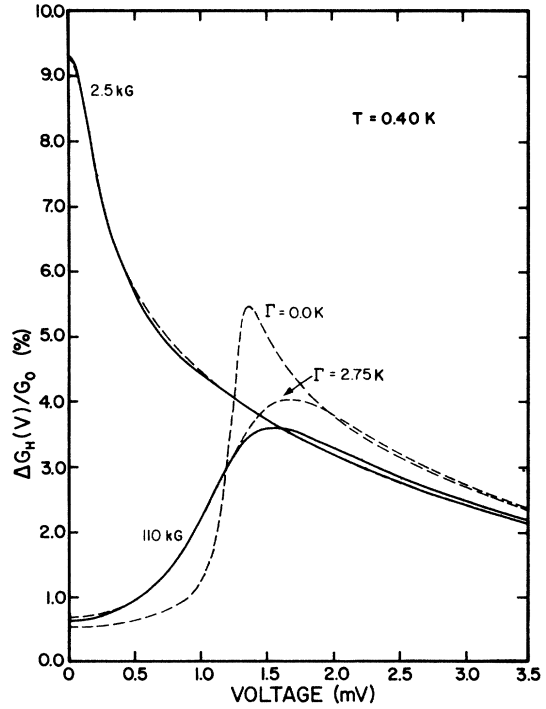

FIG. 7. Comparison of the experimental (solid) even conductance to the theoretical (dashed) WL-modified Appelbaum result for the intermediate field $H = 110$ kG and the low field $H = 2.5$ kG. The experimental background conductance has been subtracted and the difference normalized to the background conductance at zero bias, G_0. The value of the broadening parameter $\Gamma = 2.75$ K was selected to give the best fit to the slope of the well in the vicinity of $\Delta = 1.26$ meV. The value of g is 1.98, and the coefficient of the $G^{(2)}$ term is $A_2 = 6.45$ (see text). Also shown is the unsmeared Appelbaum result ($\Gamma = 0.0$) for the same value of these parameters. Note that the overshoot behavior for $eV > \Delta$ is poorly reproduced by the theory.

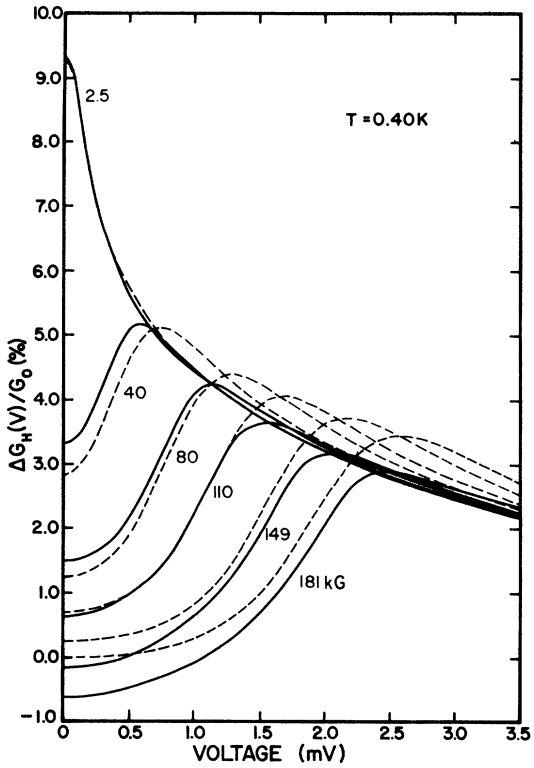

FIG. 8. Comparison of the experimental (solid) even conductance to the theory (dashed) for five fields between 40 and 181 kG using the values of g and A_2 computed from fitting the 110-kG curve as in Fig. 7. Γ for each field has been adjusted to match the slope in the vicinity of the Zeeman energy.

the slope of the well in that particular field. Even with this flexibility in changing Γ, the fit to the data is not good, with the deviations both in the depth and the width of the well becoming more marked the further away we go in field from the (arbitrary) reference curve at 110 kG. That the good fit obtained at 110 kG was not a peculiarity of that particular field curve is demonstrated in Fig. 9, where the three parameters A_2, g, and Γ (recall A_3 is fixed by the zero- or low-field curve) have been allowed to vary to give the best fit at each particular field. However, the good agreement between the solid and dashed curves for all the fields in Fig. 9 is not actually a verification of the theory, but rather indicates (along with Fig. 8) the inadequacy of the theory to account for the field dependence as the variation in the coefficient A_2 of the $G^{(2)}$ term required to achieve this match is beyond theoretical justification, i.e., there is no reason to expect the ratio of the $G^{(2)}$ term to the $G^{(3)}$ term to vary as a function of field. The required variation of A_2 is shown plotted as the dashed curve (right-hand scale) in Fig. 10 (note it goes from 3.4 at 40 kG to 8.1 at 181 kG).

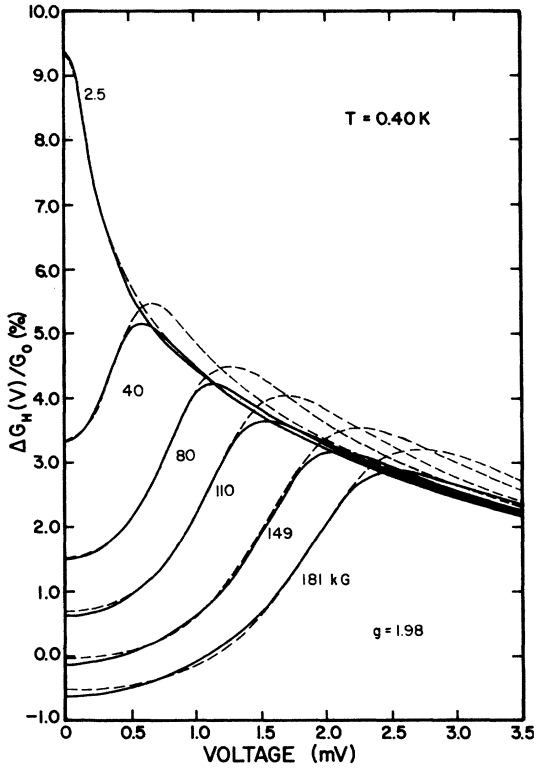

FIG. 9. Comparison of the experimental (solid) even conductance to the theory (dashed) for the same five fields as in Fig. 8, but with the respective values of g, A_2, and Γ adjusted to give the best fit to the experimental curve for that particular field. $g=1.98$ is the same for all fields, but A_2 varies from 3.39 for 40 kG to 8.09 for 181 kG (see Fig. 10), while the values of Γ are: $\Gamma(40)=1.57$ K, $\Gamma(80)=2.29$ K, $\Gamma(110)=2.75$ K, $\Gamma(149)=3.44$ K, and $\Gamma(181)=3.96$ K.

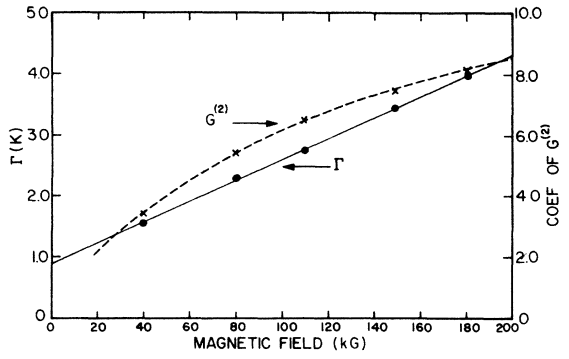

FIG. 10. Plot of the broadening parameter Γ and of the coefficient of the $G^{(2)}$ term A_2 as a function of magnetic field from the fitting procedure of Fig. 9. Note that $\Gamma(H)$ is approximately linear in field but with a large zero intercept.

An interesting aspect of the plots of Fig. 9 though is that the optimum fits at various fields were all obtained with the *same value of g*, namely, $g=1.98$. That this is more than fortuitous is additionally indicated by the plot in Fig. 11 (solid circles) of the voltages at which, for each field, dG/dV is a maximum. These points, used in previous work[3,12,26] to define $\Delta = g\mu_B H$, fall in our case on a straight line but with a nonzero intercept.

The straight line (shown dashed in Fig. 11) of the same slope, but displaced upward by 0.14 mV so that it passes through the origin, is described by the equation $eV = g\mu_B H$ with g similarly equal to

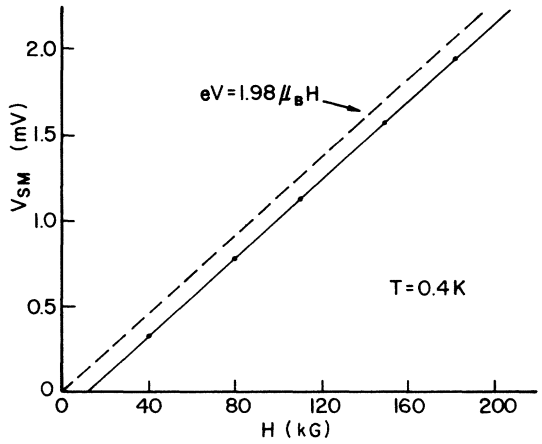

FIG. 11. Plot of the voltages (solid circles) V_{SM} at which the slope of the conductance well is a maximum vs field. Dashed curve is straight line of same slope but passing through the origin and corresponds to the value of g obtained by the curve-fitting procedure of Fig. 9.

1.98. We have already discussed how using the voltage of dG/dV_{max} underestimates Δ in theory; in a careful determination, the same is evidently true experimentally. It is reasonable to suggest that the theory, although imperfect, may be used in a parametrized form to generate empirical curves to match to experiment so as to recover useful values of those parameters like g and Γ.

A natural question arises as to whether an equally good fit to the data as shown in Fig. 9 could be obtained with a substantially different value of g by using another procedure to vary the parameters. The result of using such a different procedure is shown in Fig. 12, for values of g that represent a $\pm 10\%$ change from 1.98. Here the width of the well in the region of steepest slope is fitted by adjusting the size of $G^{(2)}$, and the slope itself by adjusting Γ as done previously. The degradation in the fit even for this rather small variation in g is quite marked. Our studies indicate that a variation in g of no more than $\pm 3\%$ can be tolerated before the quality of the fit in Fig. 9 deteriorates noticeably.

The values of the broadening parameter Γ as a function of field derived from the fitting procedure of Fig. 9 are shown as the solid circles in Fig. 10 (left-hand scale). Γ does vary approximately linearly with field as shown by the straight line drawn through the points but the zero-field intercept is quite large (0.9 K), when it should be zero.

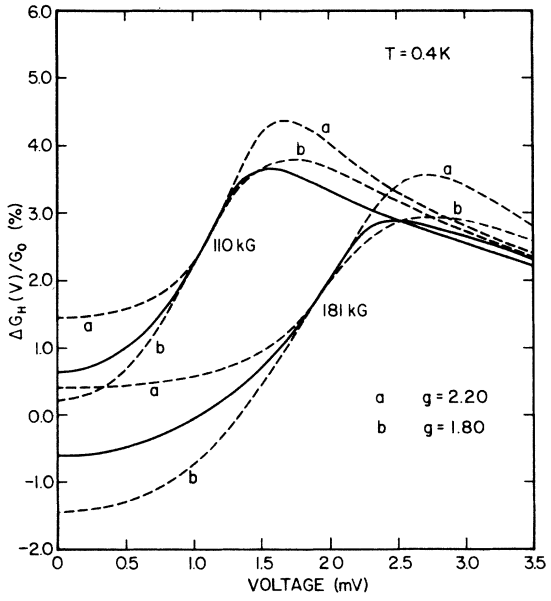

FIG. 12. Comparison of the experimental (solid) even conductance for $H = 110$ and 181 kG with theoretical (dashed) conductances calculated using an alternate fitting procedure (see text) for values of g that represent a $\pm 10\%$ deviation from best-fit value of g obtained from Fig. 9.

The slope of the line in Fig. 10 is 0.0170 K/kG. Disregarding the nonzero intercept and assuming this slope measures Γ/Δ in Eq. (6), we calculate a value for Γ/Δ of 0.127 using $g = 1.98$. From Eq. (6) we find then that the required value of $J\rho$ is -0.201. Now from Eq. (7), which gives $J\rho$ in terms of the g shift, we calculate $J\rho = -0.04$ using $g_0 = 2$ and $g = 1.92$, which value of g represents the lower limit in our fitted value of $g = 1.98 \pm 3\%$. The two values differ by a factor of 5. A g value of 1.6, substantially beyond our limit of experimental error, would be required to produce agreement. Using the slope of the line in Fig. 10 to estimate Γ/Δ represents a lower limit for this quantity. Simply taking the ratio of Γ to H at any given field (e.g., at the maximum field (181 kG), $\Gamma/H = 0.165$) increases Γ/H and consequently $J\rho$, and further worsens the agreement between $J\rho$ calculated from Eqs. (6) and (7). Simply put, the relatively small observed g shift cannot adequately account for the measured broadening of the high-field curves.

C. Temperature dependence

The values of the broadening parameter Γ were deduced from measurements at the lowest temperature 0.4 K, to minimize the smearing effects of T itself. Even at 40 kG, the deduced value of Γ of 1.57 K significantly exceeds T, and thus $kT^* \simeq \Gamma$. It is interesting to compare the experimental curves at a higher temperature to the theory with all the parameters deduced at 0.4 K left unaltered. Such a plot is shown in Fig. 13 for $T = 1.25$ K. The fit is about as good as that achieved at 0.4 K in Fig. 9. For the higher fields, the broadening is already quite large (e.g., $\Gamma_{149} = 3.44$ K) compared to the temperature difference between 0.4 and 1.25, and only a slight change in the curve is observed. A more substantial change occurs for the lower-field curves ($\Gamma_{40} = 1.57$ K) and provides a better test. This lower-field behavior (for 40 and 80 kG) is more clearly indicated in Fig. 14 where theory and experiment are plotted together for *both* temperatures. The approximate doubling of the slope of the side of the well and the increase in the depth of the well at 40 kG on going from 1.25 to 0.4 K is nicely accounted for by a Γ of 1.57 K and Eq. (20). The change at 80 kG is less, but still reproduced by the theory. To see significant modification in the high-field curves a larger temperature change is required. The effect of such a larger change—from 0.4 to 4.2 K—is also shown in Fig. 14 for $H = 149$ kG. Since 4.2 K is actually larger than $\Gamma_{149} = 3.44$ K, most of the smearing at 4.2 K is accounted for by the elevated temperature itself. For this case $T^* = 5.43$ K. Again the fit at the two temperatures is reasonably good, at least in the

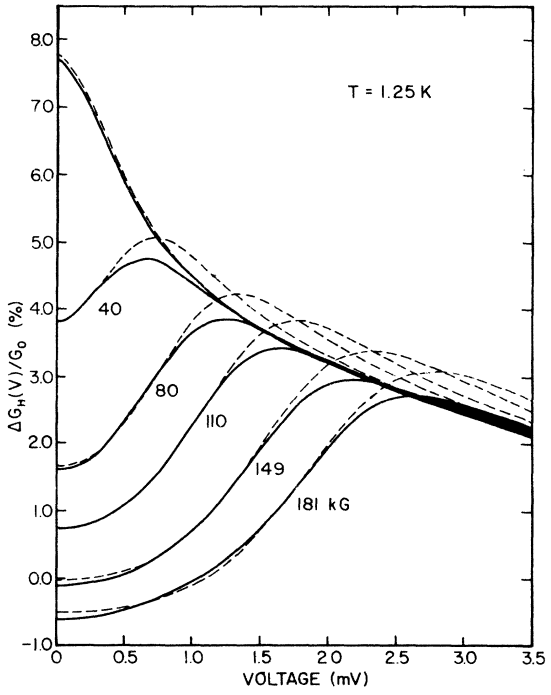

FIG. 13. Comparison of the experimental (solid) even conductance for $T = 1.25$ K to the theoretical (dashed) curves calculated using the same values of g, Γ, and A_2 obtained by fitting the magnetic field curves at the lower temperature $T = 0.40$ K as in Fig. 9.

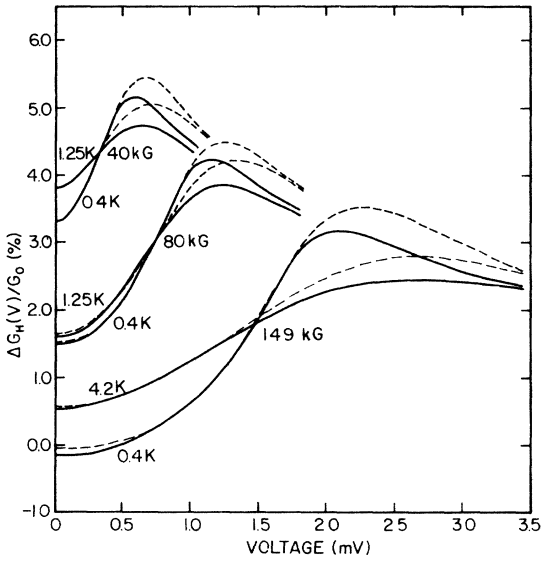

FIG. 14. Comparison of the experimental (solid) even conductance with the theoretical (dashed) conductances for two different temperatures at each of the given fields using the values of Γ from the fit at 0.4 K. The higher the field the larger the temperature change required to observe a significant change in the curve.

sensitive lower portion of the well. As before, the greatest discrepancy occurs at higher voltages in the region of the overshoot. Thus we see that the inclusion of a broadening parameter in Appelbaum's theoretical expressions can account in a quantitative manner for the change in the shape of the conductance well with temperature at a given field. That this smearing, although apparently increasing with field, is attributable to the type of magnetic-field-induced exchange broadening discussed by Wolf and Losee[12] is far from certain, however.

D. Zero-bias conductance

In Fig. 8, where theory and experiment are compared without the artifact of allowing the ratio of $G^{(2)}$ to $G^{(3)}$ to vary, we see that the greatest discrepancy in the two sets of curves occurs at zero bias. The experimental magnetic field dependence of the conductance at zero bias is shown plotted (solid line) in Fig. 15. As has been previously noted[3,12] the most unusual feature of this curve is the lack of saturation at high fields. At 181 kG and 0.4 K, $g\mu_B H/kT \simeq 60$, and the curve should be essentially flat; yet it is continuing to fall almost linearly at 180 kG at the rate of ~0.3% for every

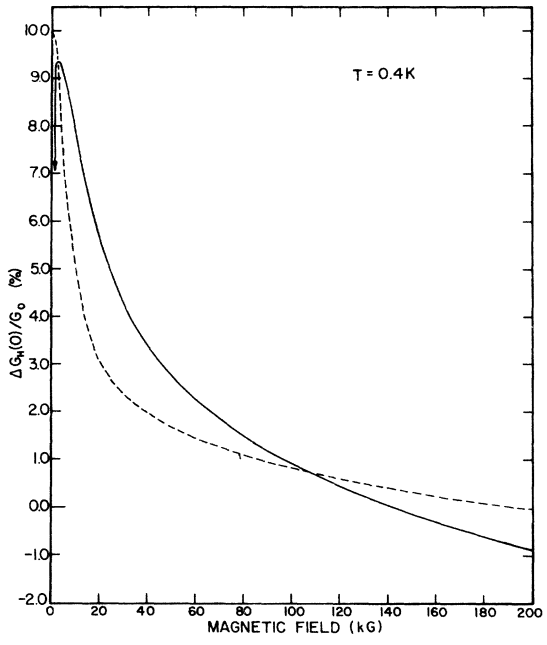

FIG. 15. Plot of the experimental (solid) magnetoconductance at zero bias and 0.40 K as a function of field compared to the theory (dashed) obtained by assuming a strictly linear relation between Γ and H using the value of Γ obtained from the fit to the 110-kG curve (see text). Beyond 180 kG the experimental curve is extrapolated. Note the lack of saturation of the experimental curve at the highest fields.

20 kG. To determine whether the inclusion of the magnetic-field-induced lifetime broadening might account for the observed zero-bias magnetoconductance, we have used the broadening parameter calculated from the slope of the well at the intermediate field of 110 kG ($\Gamma = 2.75$ K) to define a strictly linear relation between Γ and H of the form

$$\Gamma = (2.75/110)H = 0.025H,$$

in accord with Eq. (6). Compared to the $\Gamma(H)$ function exhibited in Fig. 10, this actually overestimates the smearing (and thus the tendency toward saturation) for $H > 110$ kG. Taking the value of A_2 used to fit the curve at 110 kG, we calculate the dashed line in Fig. 15. The fit to the experimental curve is poor, with the theoretical conductance falling much more sharply at low field than the observed conductance, and failing to reproduce the lack of saturation of the conductance at high field.

IV. CONCLUSION

The results have been presented of an extremely careful study of the zero-bias conductance peak in a Fe-doped Al-I-Al tunnel junction in fields up to 181 kG and at temperatures down to 0.4 K. In zero field, the voltage and temperature dependences of the peak conform closely to the predictions of the Appelbaum-Kondo[15,16] theory, providing a direct measure of the Kondo scattering amplitude in the perturbational limit. We find, however, that in a magnetic field the Appelbaum theory, even including the exchange broadening suggested by Wolf and Losee,[12] cannot adequately account for the observed experimental behavior. While, for a given magnetic field, it is possible with a suitable adjustment of the parameters such as the g factor, the lifetime broadening Γ, and the relative sizes of the $G^{(2)}$ and $G^{(3)}$ to fit the lineshape over a substantial portion of the field-induced conductance well, it is not possible without varying the size of $G^{(2)}$ to fit the lineshape at other fields. In no instance can the theory, using reasonable values of the parameters deduced from the fit to the well, reproduce the small amount of overshoot observed experimentally for $eV > \Delta$.

From our curve-fitting procedure we deduce consistent values of g and Γ that we consider are more reliable from the standpoint of properly parametrizing the theory than those obtained by merely locating various critical points such as dG/dV_{max} and $dG/dV = 0$. We find that the measured broadening parameter Γ increases with the field in an approximately linear fashion, but extrapolates to a large nonzero intercept at $H = 0$. Furthermore, the size of the coupling parameter $J\rho$ required to fit the slope of the Γ vs H curve is approximately five times larger than the value of $J\rho$ computed from taking the largest possible g shift permitted by our experimental uncertainty. Thus, while a broadening that increases as the magnetic field increases clearly does exist in M-I-M junctions, its behavior is not consistent with the expressions [Eqs. (6) and (7)] which constitute the basic result of the Wolf and Losee theory. Whatever the origin of the broadening, its inclusion is necessary to account for the temperature dependence of the experimental curves at a given field. The values of Γ obtained from fitting the voltage line shape at low temperature (0.4 K) quantitatively account for the observed dependence of the curves on temperature, at least in the central portion of the well.

The broadening observed in M-I-M tunnel junctions may not necessarily be a feature of all types of tunnel junctions exhibiting conductance peaks. The rigorously triangular well,[14] exhibiting a cusp at zero bias, observed in metal-semiconductor tunnel junctions at high field and very low temperatures is not consistent with any large degree of field-induced broadening; nor is the quite sharp temperature dependence observed for such a well below 1.25 K. Lastly, the observed zero-bias magnetoconductance in our samples is in serious disagreement with the theory for any reasonable choice for the dependence of the broadening on field. The lack of saturation of the magnetoconductance at fields as high as those used in this study remains one of the least understood aspects of the magnetic field behavior of the conductance peak.

Another explanation for the observed well shapes, originally suggested by Rowell and Tsui[13] in connection with the roughly triangular well they observed in Schottky-barrier junctions, was a distribution of g values. A possible justification for such a distribution could come from Eq. (6), $g = g_0 + 2J\rho$, where, for impurities distributed throughout the insulator, the coupling constant J would become a function of the distance of the impurity from the metal interface, and produce a spread of g values. The rigorously triangular well[14] observed in the semiconductor junctions would, however, require an essentially uniform distribution of g values all the way down to zero with a corresponding $J\rho$ value at that point of unity. This seems extremely unlikely. Wallis and Wyatt[26] have considered the effect of such a range of g values in their M-I-M junctions, possibly caused by crystal-field effects in the insulator. There is no evidence from electron-spin-resonance studies, or any studies for that matter, that the spread of g values they employ (uniform from $g = \frac{1}{3}$ to 2) to

improve the fit to his data is a justifiable one. We have seen in this work that just by utilizing *three* parameters we can fit the experimental curves over wide ranges of field and temperature. The increased flexibility in fitting the data inherent in using an essentially infinite number of parameters available from an arbitrary distribution of g's is obvious. Our approach in this paper has been to carefully compare the experimental behavior to theory that already exists and which is based on reasonable foundations. While it is possible that a distribution of g values may be able to account for the smearing of the well and the behavior of the magnetoconductance, without independent evidence indicating what this distribution might be, an approach using an arbitrary distribution seems to us to be of limited usefulness.

Rather, at this point, one should look to an improvement in the theory. In particular, an extension of Appelbaum and Brinkman's[17] much more rigorous Green's function treatment or, better yet, of Ivezic's[23] hopping-model approach to include the effect of a magnetic field would be very welcome.

ACKNOWLEDGMENTS

We should like to thank Dr. R. Meservey for his encouragement and support of this work. This work was supported in part by the NSF under Grant No. DMR 76-17379 and the PSC-BHE Research Award Program of The City University of New York.

[1]A. F. G. Wyatt, Phys. Rev. Lett. 13, 401 (1964).
[2]L. Y. L. Shen and J. M. Rowell, Phys. Rev. 165, 566 (1968).
[3]J. A. Appelbaum and L. Y. L. Shen, Phys. Rev. B 5, 544 (1972).
[4]F. Mezei, Phys. Lett. 25A, 534 (1967).
[5]P. Nielsen, Solid State Commun. 7, 1429 (1969).
[6]R. C. Morris, J. E. Christopher, and R. V. Coleman, Phys. Lett. 30A, 396 (1969).
[7]S. Bermon and M. Ware, Phys. Lett. 35A, 226 (1971).
[8]A. F. G. Wyatt, J. Phys. C 7, 1303 (1974).
[9]D. J. Lythall and A. F. G. Wyatt, Phys. Rev. Lett. 20, 1361 (1968).
[10]A. F. G. Wyatt and R. H. Wallis, J. Phys. C 7, 1279 (1974).
[11]R. H. Wallis and A. F. G. Wyatt, Phys. Rev. Lett. 29, 479 (1972).
[12]E. L. Wolf and D.L. Losee, Phys. Rev. B 2, 3660 (1970); Phys. Rev. Lett. 23, 1457 (1969); Solid State Commun. 7, 665 (1969); Phys. Lett. 29A, 334 (1969).
[13]J. M. Rowell and D. C. Tsui, Bull. Am. Phys. Soc. 16, 419 (1971).
[14]S. Bermon, N. A. Mora, and J. L. Smith, Bull. Am. Phys. Soc. 18, 356 (1973); also pp. 73–75 of the review article by E. L. Wolf, in *Solid State Physics*, Vol. 30, edited by F. Seitz, D. Turnbull, and H. Ehrenreich (Academic, New York, 1975).
[15]J. Kondo, Prog. Theor. Phys. (Jpn.) 32, 37 (1964).
[16]J. A. Appelbaum, Phys. Rev. 154, 633 (1967).
[17]J. A. Appelbaum and W. F. Brinkman, Phys. Rev. B 2, 907 (1970).
[18]J. A. Appelbaum and W. F. Brinkman, Phys. Rev. 186, 464 (1969).
[19]A. Zawadowski, Phys. Rev. 163, 341 (1967).
[20]F. Mezei and A. Zawadowski, Phys. Rev. B 3, 167 (1971); 3, 3127 (1971).
[21]S. Bermon and C. K. So, Phys. Rev. Lett. 40, 53 (1978).
[22]J. Soloyom and A. Zawadowski, Phys. Kondens. Mater. 7, 325; 7, 342 (1968).
[23]T. Ivezic, J. Phys. C 8, 3371 (1975).
[24]C. Caroli, R. Combescot, P. Nozières, and D. Saint-James, J. Phys. C 4, 916 (1971); 5, 21 (1972).
[25]P. Nielsen, Phys. Rev. B 2, 3819 (1970).
[26]R. H. Wallis and A. F. G. Wyatt, J. Phys. C 7, 1293 (1971).
[27]M. B. Walker, Phys. Rev. 176, 432 (1968).
[28]Y. Wang and D. J. Scalapino, Phys. Rev. 175, 734 (1968).
[29]S. Bermon and D. E. Paraskevopoulos (unpublished).
[30]P. E. Bloomfield and D. R. Hamann, Phys. Rev. 164, 856 (1967).
[31]H. Suhl, Phys. Rev. Lett. 23, 92 (1969).